Stacking patterns in self-assembly opal photonic crystals

X. Checoury
Institut d'Electronique Fondamentale, Université Paris-Sud, UMR8622, Orsay F-91405, France and CNRS, Orsay F-91405, France

S. Enoch
Institut Fresnel, UMR CNRS 6133, Faculté des Sciences et Techniques, Case 161, 13397 Marseille Cedex 20, France

C. López and A. Blanco[a)]
Instituto de Ciencia de Materiales de Madrid (CSIC) and Unidad Asociada CSIC-UVigo, C/Sor Juana Inés de la Cruz 3, 28049 Madrid, Spain

(Received 30 January 2007; accepted 18 March 2007; published online 20 April 2007)

In this letter the authors present both experimental and numerical studies of the optical properties of four-layer artificial opals. The stacking of four layers of spheres may arise according to three different arrangements: face-centered cubic, hexagonal close packed, or double hexagonal close packed. The study shows that the transmission spectra features are characteristic of the type of stacking, and thus, each color region observed under the optical microscope can be unambiguously associated with one of the stacking types. © *2007 American Institute of Physics*.
[DOI: 10.1063/1.2724916]

Three-dimensional photonic crystals (PhCs) are attractive optical materials for achieving a fine control of light propagation in all the space directions. Currently, self-organized synthetic opals are considered as good and inexpensive candidates for the fabrication of PhC with interesting properties in the optical range.[1] Methods for opal fabrication rely on the tendency of colloidal particles to self-assemble in various ordered and close-packed structures. These resulting structures usually consist in a stacking of hexagonal close-packed monolayers of spheres. Unfortunately, the methods of fabrication cannot avoid some sort of disorder in this stacking. To describe the stacking pattern, it is usual to denote each possible position of the hexagonal close-packed monolayers by one of the three letters A, B, and C. The fabricated structures may be a face-centered cubic (fcc) structure with a repeating ABC pattern or a hexagonal close-packed (hcp) structure with a repeating AB pattern.[2] Other patterns like the double hexagonal closed-packed (dhcp) pattern of type ABCB or random patterns can also be present. The optical properties of these different structures may be quite different and have already been the subject of various studies.[3–5] In these studies, it appears that the diffraction pattern is highly sensitive to the stacking. This dependence opens the possibility of deducing some pieces of information about the opal structure from optical measurements. A first step towards this difficult but highly desirable aim is to identify the properties of opals made with few layers since, in some cases, larger structures are likely to mainly be periodic versions of these opals with few layers.

In this letter, we study the optical properties of opals made with 1–4 ML of polystyrene spheres. We show that a simple transmission measurement along with an exact finite difference time domain (FDTD) simulation of ideal opals allows to fully determine the stacking type of three- and four-layer opals. In particular, we do not rely on this for the measurement of the diffracted power.

Thin film opals were grown with polystyrene spheres, diameter of 870 nm, by the vertical deposition method described elsewhere.[6] This configuration leads mainly to the growth of a close-packed structure in fcc configuration, but some stacking faults are usually observed. In the early stages of growth, crystal structure strongly depends on the meniscus shape, which mainly depends on experimental parameters such as temperature, concentration, and substrate surface nature, and capillary forces during drying.[7] Therefore, small variations in these conditions can lead to different crystal arrangements such as square (100) orientations or stacking faults, which are usually observed in this sort of structures.[8] Once the opaline sample reaches the final (stationary) thickness, the dominant crystal structure is fcc (Fig. 1).

Optical microscopy images of the prepared samples are shown in Fig. 2, where sample thickness (in monolayers) has been indicated. As explained below, the sample thickness can be estimated from Fabry-Pérot oscillations present in the reflection and transmission spectra on either side of the first Bragg peak. Starting from 3 ML, different stacking arrangements are possible, which provoke different hues (two different hues for 3 ML, three for 4 ML, etc., as can be seen in Fig. 2). To be specific, in this letter, we mainly study the three main stacking sequences, which are fcc, hcp, and dhcp. As a consequence, we focus our attention on the four-layer samples that may contain a representative of these three

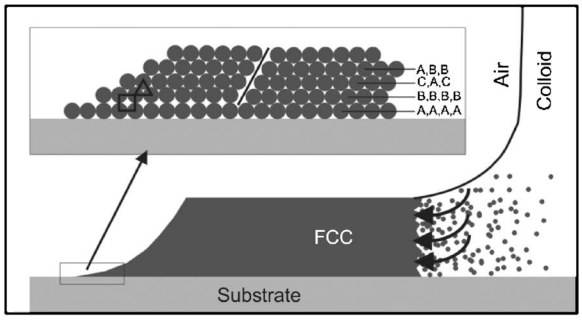

FIG. 1. Schematic diagram of the growth process. Notice that growth takes place along the substrate rather than perpendicular to it.

[a)]Author to whom correspondence should be addressed; electronic mail: ablanco@icmm.csic.es

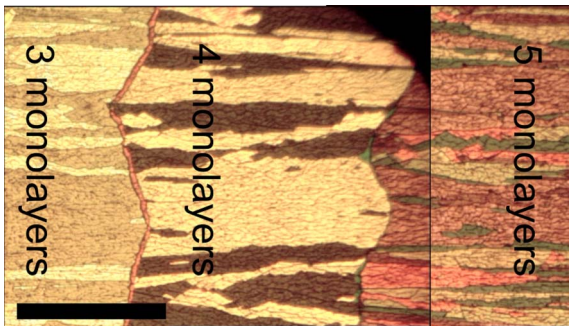

FIG. 2. (Color online) Stitched optical microscopy images showing regions with different morphologies. Scale bar is 1 mm.

stacking patterns, schematically represented in the insets of Figs. 3–5.

As seen in Fig. 2, under an optical microscope, the four-layer part presents three different colored areas: most of the surface is orange with some brown filaments. Some small areas have a rather yellow color. We expect that these different colored areas match the three stacking possibilities allowed for a four-layer opal. To confirm this hypothesis, the transmission and reflection at normal incidence of every colored area of the sample have been measured using a Fourier transform infrared spectrometer Bruker IFS 66/S attached to an optical microscope, which allows different area selection with high accuracy.

The recorded experimental wide range spectra (from 0.5 to 2.5 μm) for each area of the sample are represented by black curves in Figs. 3–5 as a function of the normalized frequency a/λ, where λ is the wavelength in vacuum and a (the lattice parameter) is equal to $d\sqrt{2}$, with d being the diameter of the spheres. All the measured spectra are typical and scale with sphere diameter, but we have chosen those covering our detection range. For normalized frequencies a/λ below 1.15, the three spectra are quite similar from one colored area to the other. In particular, a minimum of transmission always occurs near $a/\lambda=0.59$. It corresponds to the frequency location of the first pseudogap in the (111) direction in the case of a fcc structure. These results were expected since, for a/λ below 1.15, the transmission and reflection spectra at normal incidence (the Z direction in the insets) are roughly determined by the first Fourier component of the dielectric map along the direction of light incidence. This Fourier component is the same for the three patterns. As a consequence, in this frequency range, the opals roughly behave as a Bragg mirror with period $d\sqrt{(2/3)}$. In particular, the frequency of the two first gaps of this mirror can be estimated in good agreement with the experiments by

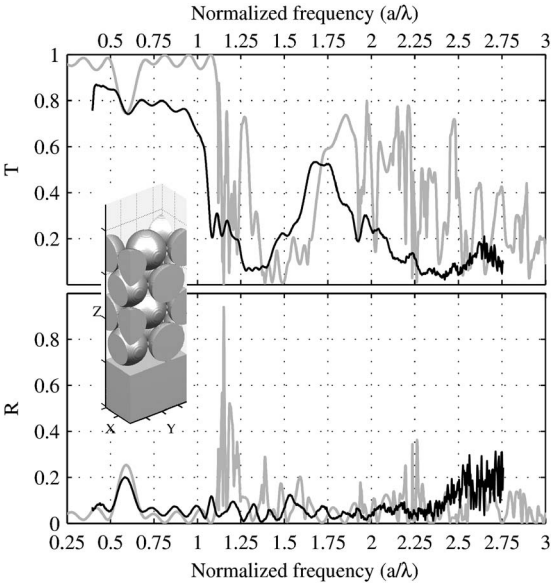

FIG. 4. Transmission (top) and reflection (bottom) spectra of a four-layer opal arranged in a hexagonal close-packed structure (i.e., with a stacking of the form ABAB). The black and gray curves represent experimental and simulated results, respectively. In both cases, the incident light is perpendicular to the stacking direction (i.e., the Z direction). Inset: schematic view of the simulated opal.

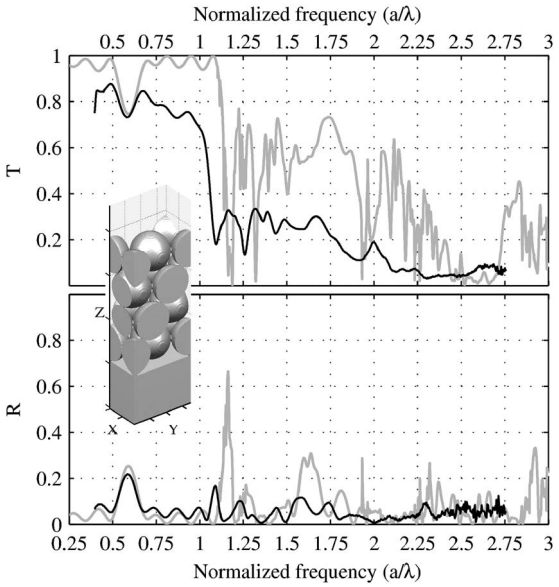

FIG. 3. Transmission (top) and reflection (bottom) spectra of a four-layer opal arranged in a face-centered cubic structure (i.e., with a stacking of the form ABCA). The black and gray curves represent experimental and simulated results, respectively. In both cases, the incident light is perpendicular to the stacking direction (i.e., the Z direction). Inset: schematic view of the simulated opal.

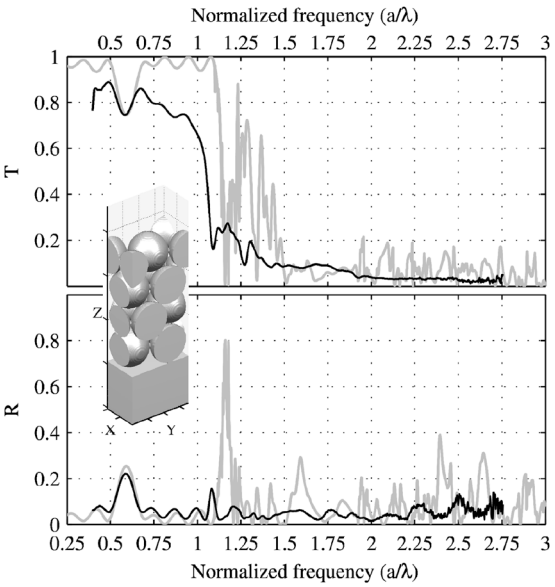

FIG. 5. Transmission (top) and reflection (bottom) spectra of a four-layer opal with a stacking of the form ABCB. The black and gray curves represent experimental and simulated results, respectively. In both cases, the incident light is perpendicular to the stacking direction (i.e., the Z direction). Inset: schematic view of the simulated opal.

$(\sqrt{3})/(2n_{\mathrm{eff}}) \approx 0.61$ and $(2\sqrt{3})/(2n_{\mathrm{eff}}) \sim 1.22$, with $n_{\mathrm{eff}}=1.42$ the average index of the opal.[9] Because all the sample area behave as the same Bragg mirror whatever the stacking pattern along the growth direction, it is quite straightforward to deduce the thickness of this mirror and thus the thickness of the sample from the Fabry-Pérot oscillations present in the spectra.

For normalized frequencies above 1.15, i.e., for the high frequency region, transmission and reflection spectra strongly differ and explain the different colors of the samples. Indeed, in this high frequency range, the transmission and reflection spectra will depend on the Fourier components of the dielectric map in all space directions. These components strongly depend on the stacking pattern. In Figs. 3–5, the transmission spectra clearly show three different tendencies for a/λ above 1.25. In Fig. 3 an average transmittance is observed in the frequency range from 1.25 to 1.75, while a very low transmittance is observed in Fig. 5 above 1.25. On the contrary, a transmission peak appears around $a/\lambda \approx 1.75$ in Fig. 4. Although reflection spectra are also different from one colored area of the sample to another, they remain more difficult to describe.

To verify that the three regions of the sample really correspond to three different stacking patterns of the four-layer opals, three-dimensional FDTD simulations have been carried out. The simulated opals are periodic in the X and Y directions and finite in the third one (see insets of Figs. 3–5). Perfectly matched layer boundary conditions terminate the simulation domain in the Z direction. The simulation parameters used for the four-layer opals are the same as the experimental ones. The polystyrene spheres have a refractive index of 1.57 and a diameter d of 870 nm. They lie on a glass substrate with a refractive index of 1.45. The FDTD space step (dx) is equal to $d/41=21$ nm, and the time step (dt) is equal to $dx/(2c)=3.5\times10^{-5}$ ps. For the sake of simplicity, neither absorption nor frequency-dependent refractive indices are included in the model. The incident field is a plane wave propagating along the direction Z towards the substrate. The field is recorded on two planes respectively located in the air and the substrate at 210 nm from the opal edge. Instead of the Fourier transform, the Padé approximant technique[10] is used on the recorded time-domain data to accurately determine the spectra of the electromagnetic field without requiring the long-time evolution of it. Finally, a near-field to far-field transform is applied to get the reflectance and transmittance of the opals from these fields.[11] The overall simulation time is below 1.5 h on a desktop computer.

Despite the relative simplicity of the model, the overall characteristics of the simulated spectra are in good agreement with the measured ones (Figs. 3–5). Because the model consists in a perfectly periodic structure made of smooth spheres, resonances are much sharper in the simulation than in the measurement. Indeed, in real opals, sphere roughness as well as small variation in diameter lead to some scattering that is not taken into account by the model. The effect of this supplementary scattering is similar to additional losses[12] and smooths the curves significantly. For example, in the low frequency range $(a/\lambda \approx 1.25)$, the sum of the experimental reflectance and transmittance is between 0.8 and 0.95, whereas it is equal to 1 rigorously in the simulation. Other sources of discrepancy are, on one hand, the frequency varying refractive index of the polystyrene spheres (~3% in this frequency range) that is responsible for the frequency shift in the high frequency region between simulated and measured data or, on the other hand, very small lattice variations which will have higher effects at higher energies. Nevertheless, it is possible to qualitatively match the spectra of fabricated opals and the simulated ones. The simple model of a perfectly periodic opal is sufficient to unambiguously identify the stacking of every area of the sample. As seen, the measured spectra of Fig. 3 correspond to the simulated spectra of a fcc structure. Similarly, the spectra of Figs. 4 and 5 correspond to those of a hcp structure and a dhcp structure, respectively.

Similar agreements between simulated and measured spectra have been obtained for one-, two-, and three-layer opals. In particular, it is possible to determine the stacking pattern of a three-layer opal from its transmission spectra without the need for measuring the diffraction pattern.

In conclusion, we have presented a detailed comparison between experimental transmission and reflection spectra of up to four-layer artificial opals made of polystyrene spheres. FDTD calculations have allowed us to show that the three possible stackings, namely, fcc, hcp, and dhcp, can be unambiguously identified and associated with the observed domains of different colors. Indeed, the transmission spectra for the shorter wavelengths have been shown to present features characteristic of each stacking. These features can be very faithfully modeled by the calculation even with no adjustable parameters. Inclusion of spectral dispersion and geometric detail allows nearly perfect fits of the spectra. This result may have important repercussions for the control of the quality of the opals.

A precise study of the consequences of the deviations of the opals from the perfect periodic media is certainly one of the most challenging goals in the domain of photonic crystals but also certainly is the necessity to improve their optical quality. This study is a step towards this aim, and studying the effect of roughness and other imperfections are necessary following steps.

The support of the EC-funded projects PhOREMOST (No. FP6/2003/IST/2-511616) and Spanish MEC through Contract No. MAT 2006-09062 is gratefully acknowledged. A.B. acknowledges the *Ramón y Cajal* program.

[1] C. López, J. Opt. A, Pure Appl. Opt. **8**, R1 (2006).
[2] C. Kittel, *Introduction to Solid State Physics*, 7th ed. (Wiley, New York, 1996), Chap. 1, p. 1.
[3] Y. A. Vlasov, V. N. Astratov, A. V. Baryshev, A. A. Kaplyanskii, O. Z. Karimov, and M. F. Limonov, Phys. Rev. E **61**, 5784 (2000).
[4] Z. L. Wang, C. T. Chan, W. Y. Zhang, Z. Chen, N. B. Ming, and P. Sheng, Phys. Rev. E **67**, 016612 (2003).
[5] A. V. Baryshev, V. A. Kosobukin, K. B. Samusev, D. E. Usvyat, and M. F. Limonov, Phys. Rev. B **73**, 205118 (2006).
[6] P. Jiang, J. F. Bertone, K. S. Hwang, and V. L. Colvin, Chem. Mater. **11**, 2132 (1999).
[7] S. Maenosono, C. D. Dushkin, Y. Yamaguchi, K. Nagayama, and Y. Tsuji, Colloid Polym. Sci. **277**, 1152 (1999).
[8] P. D. Garcia, J. F. Galisteo-Lopez, and C. López, Appl. Phys. Lett. **87**, 201109 (2005).
[9] P. Yeh, *Optical Waves in Layered Media* (Wiley, New York, 2005), Chap. 6, p. 118.
[10] Q. Chen, Y.-Z. Huang, W.-H. Guo, and L.-J. Yu, Opt. Commun. **248**, 309 (2005).
[11] A. Taflov, *Computational Electrodynamics: The Finite-Difference Time-Domain Method* (Artech House, Boston, 1995), Chap. 8, p. 349.
[12] H. C. van de Hulst, *Light Scattering by Small Particles* (Dover, New York, 1987), Chap. 9, p. 114